

The 1911 M~6.6 Calaveras earthquake: Focal mechanism and relationship to static and dynamic Coulomb stress changes imparted by the 1906 San Francisco earthquake

by Diane I. Doser, Kim B. Olsen, Fred F. Pollitz, Ross S. Stein, and Shinji Toda*

Abstract We have used all available first motion, body wave and surface wave data to explore possible focal mechanisms for the 1 July 1911 Calaveras earthquake. We find that the 1911 event was most likely a right-lateral strike-slip Calaveras fault earthquake, larger than but otherwise resembling the 1984 M=6.1 Morgan Hill earthquake in roughly the same location. We could recover, however, no unambiguous displacement or strain data to corroborate the seismic analysis. The occurrence of a right-lateral strike-slip event in 1911 is inconsistent with the calculated -0.4 to -3.0 bar stress decrease imparted by the 1906 rupture at that location on the Calaveras fault, and 5 years of calculated post-1906 viscoelastic rebound does little to reload the Calaveras fault. We also calculated the peak dynamic Coulomb stress imparted by the 1906 rupture, and find that the 1911 shock struck where the dynamic stress increased by 1-6 bars. Despite this positive association between the dynamic stress and the 1911 earthquake, there is no correlation of 1906 aftershock frequency or magnitude with the peak dynamic stress, perhaps because the sample is small and the aftershocks are poorly located. Just 20 km to the south of the 1911 epicenter, surface creep of the Calaveras at Hollister paused for ~17 years after 1906, about the expected delay for the calculated static stress drop imparted by the 1906 earthquake when San Andreas postseismic creep and viscoelastic relaxation are included. Thus, the 1911 Calaveras earthquake may have been promoted by the transient dynamic stresses, while Calaveras creep was inhibited by the static stress changes.

*Order of authorship is alphabetical; all contributions are equal.

Introduction

The 1906 San Francisco earthquake is calculated to have reduced the static stress along adjacent, sub-parallel, strike-slip faults in the greater San Francisco Bay area (Figure 1) (Simpson and Reasenberg, 1994; Harris and Simpson, 1998). Although contested by Felzer and Brodsky (2005), this 1906 'stress shadow' has been invoked by Simpson and Reasenberg (1994), Harris and Simpson (1998), Stein (1999), and Pollitz et al (2004) to explain the roughly order-of-magnitude drop in the rate of $M \geq 6$ shocks in the Bay area in the 75 years following the 1906 earthquake. In contrast to 14 such events in the 75 years preceding 1906, only one $M \geq 6$ event, the 1911 Calaveras earthquake, struck in the 75 years after the 1906 earthquake. At least three studies (Jaumé and Sykes, 1996; Harris and Simpson, 1998; Hori and Kaneda, 2001) analyzed why the 1911 earthquake might have occurred in the 1906 stress shadow. Harris and Simpson (1998) and Hori and Kaneda (2001) argued that the 1906 earthquake might have delayed the 1911 event by up to five years, either because it was about to rupture in 1906, or because of the high Calaveras creep rate. Jaumé and Sykes (1996) argued that the 1911 event could have struck on a thrust fault oriented parallel to the Calaveras fault, in which case the 1906 stress changes would be positive, promoting failure. It is thus necessary to determine the focal mechanism, location, and magnitude of the 1911 event, since the sign and magnitude of stress change are dependent on the geometry, location, and rake of the receiver fault.

Here we use first motion, regional and teleseismic waveforms of the 1911 event to determine its focal mechanism and improve its magnitude estimation. We then resolve the static and dynamic stress changes imparted by the 1906 shock on the fault plane interpreted from this mechanism. Our conclusions are tempered by the limited low-quality seismic, surface displacement and geodetic data, but suggest that the event was right-lateral, and was most likely triggered by dynamic, rather than static, stress changes.

Previous Studies

The initial studies of the 1911 Calaveras earthquake summarized mainshock and aftershock arrival times (Wood, 1912a), intensities (Templeton, 1911), earthquake damage and instrumental and human perceptions (Oldenbach, 1911). No reports of surface faulting accompanied the earthquake, although damage reports were later interpreted to indicate a rupture on the Calaveras fault. Gutenberg and Richter (1954) assigned the event a magnitude 6.6 and Ellsworth (1990) an M_S of 6.5.

Oppenheimer et al. (1990) used Wood's travel times to relocate the 1911 aftershocks under the assumption that they occurred along the Calaveras fault, concluding that 1911 aftershocks occurred on same section of the Calaveras fault as did aftershocks of the $M=6.1$ April 24, 1984 Morgan Hill mainshock. By comparing intensities for the 1984 and 1911 events, Topozada (1984) concluded that both events had the same magnitude and occurred on overlapping segments of the Calaveras fault. Bakun (1999) reanalyzed the intensity data and found it to be consistent with Calaveras fault rupture in a location similar to that of the 1984 mainshock. He estimated a moment-magnitude of 6.2 (+0.2,-0.3 units) for the mainshock.

Seismic Data

In an attempt to improve the constraints on focal mechanism and magnitude of the 1911 mainshock, we collected first-motion information from instrumental records and from the literature, and obtained all still-extant seismograms for the event. Sadly, nearly all observations from the numerous Jesuit seismic observatories in the United States have been lost. But fortuitously, we were able to obtain seismograms at two stations that recorded both the 1911 and 1984 events. In one case (Göttingen) the seismograms were recorded by instruments that had very similar responses in 1911 and 1984 (Table 1).

Seismic Analysis

First motions

P-waves for the 1911 mainshock were visible only at stations located in central California (Figure 2). The record for the Los Gatos seismoscope (GAT) is published in Oldenbach (1911). First motions for Mt. Hamilton (MHC) and Santa Clara (SCL) were read from copies of the original seismograms. Ground motion information for Berkeley (BRK) was obtained from Wood (1912b). While these data are consistent with a strike-slip mechanism similar to that of the 1984 Morgan Hill earthquake, they are not sufficient to distinguish between strike-slip and reverse mechanisms.

Body waves

Few instruments with sufficient gain to record a magnitude 6.0-6.5 earthquake were operating in the world in 1911. After an extensive search we were able to obtain S waveforms recorded at St. Louis Missouri (SLM, $\Delta=25^\circ$), Göttingen (GTT, $\Delta=82^\circ$) and Debilt (DBN, $\Delta=80^\circ$). In contrast, no S waves were observed at either GTT or DBN for

the 1984 Morgan Hill earthquake. We modeled waveforms with the technique of Baker and Doser (1988), modified by Doser and VanDusen (1996). Simple crustal velocity models were used at the source (30-km thick crust with $V_p=6.3$ km/sec and $V_s=3.6$ km/sec over a mantle with $V_p=8.0$ km/sec and $V_s=4.2$ km/sec) and receivers (35-km thick crust with the same velocities as the source model). The modeling indicates that the SH waveform shapes and polarities match synthetic seismograms for a strike-slip mechanism similar to the 1984 Morgan Hill earthquake (strike= 320° , dip= 88° , rake= 178° ; rms fit=1.78) (Figure 3) better than a reverse mechanism with an orientation similar to seismogenic structures observed just west of the Calaveras fault (Manaker et al., 2005) (strike= 320° , dip= 80° , rake= 90° ; rms fit=2.77). With the limited number of seismograms available we cannot adequately invert for a focal mechanism; however forward modeling suggest the focal mechanism uncertainties ($325^\circ\pm 25^\circ, 88^\circ\pm 5^\circ, 175^\circ\pm 5^\circ$ based on matching waveform polarities) shown in Figure 3, assuming a strike-slip starting model, with a moment magnitude of 6.6 ± 0.2 .

Surface waves

Figure 4 shows the surface waveforms recorded at DBN and GTT in 1911 and 1984. The seismograms at GTT (Figure 4a) were recorded with nearly identical instruments (Table 1). Note the similarities in waveform shape between the two events, although the amplitudes for the 1911 waveforms are a factor of ≤ 5 larger. Waveforms for the 1911 and 1984 earthquakes recorded at DBN also show similar characteristics (Figure 4b), although instrument responses differ (Table 1).

Static Coulomb Stress and Boundary Element Analysis

We calculate that the 1906 earthquake imparted a 2-4 bar left-lateral static shear stress change on the Calaveras fault at the site of the future 1911 earthquake (Figure 5 and Figure 1b). We use the Wald et al (1993), Thatcher et al. (1997), and Song et al (2007) source models for the 1906 earthquake in an elastic half space (Figure 6). By comparison, Harris and Simpson (1998) calculated a 2.0-bar stress change. The Wald et al. slip model, in part constrained by seismic records from the earthquake, contains a concentration of slip in Sonoma and southern Mendocino Counties as well as on the San Francisco Peninsula and into southern Marin County toward the North (Figure 6). In contrast, the Thatcher et al. and Song et al. models are smoother, with significant slip from Point Arena to the North and Hollister to the South. The slip profiles shown in Figure 6 were extended to the bottom of the vertical fault plane (12 km for the Wald et al. and Song et al. models, and 10 km for the Thatcher et al. model).

All three static-CFF distributions (Figure 5) yield a Coulomb stress decrease at the site of the 1911 event. The Thatcher et al. (-2 bars) and Song et al. (-3 bars) models yield the largest decreases; the Wald et al. model (-0.4 bars) is the smallest. In the absence of Calaveras creep, the Calaveras fault has been calculated to have a stressing rate of up to 0.09 bars/yr (Pollitz et al, 2004; Parsons, 2006), which means that for the Wald et al. model a delay as brief as 5 years would be possible. However, geodetic data used in the Thatcher et al and Song et al models require greater 1906 slip on the San Andreas near the 1911 epicenter than in the Wald et al model, making this short time to failure unlikely. Hollister, whose 100-year surface creep record is used for this study, has static-CFF of -2 bars for Thatcher et al., and -5 bars for Song et al., and 0.03 bars for

Wald et al.

Estimating the Calaveras earthquake delay associated with the 1906 stress shadow

We next performed a boundary element analysis to estimate the amount of left-lateral displacement (or ‘back slip’) that would be needed to shed the stress imposed by the 1906 earthquake. Here we treat the Calaveras fault as a surface of freely slipping boundary elements, in a manner similar to the Toda and Stein (2002). The amount of back slip depends not just on the magnitude of the stress change at the 1911 site, but also on the geometry and distribution of stresses along the entire fault, since the longer and straighter the fault, the more it will slip in response to a given stress change. We find that 350 ± 50 mm of left-lateral slip would be needed to relieve the imposed stress (Figure 7). Given the long-term 15 ± 3 mm/yr slip rate on this section of the Calaveras (U.S. Geological Survey, 2007), the slip deficit would be removed in 23.3 ± 0.25 years. Instead, the 1911 earthquake struck after just 5 years, long before the stress drop imparted by the 1906 shock is likely to have been erased by stress accumulation.

The ratio of the 1906 stress drop on the Calaveras fault to the long term stressing rate of the Calaveras furnishes a complementary way to estimate the expected delay of Calaveras earthquakes. The stressing rate is influenced by the stress contribution from other faults within about 30 km of the 1911 site, such as the southern Hayward and San Andreas. So we used an interseismic stressing model in which locked faults are treated as virtual dislocations (they are slipped backwards at their long term rates) over their locked width in an elastic half space. We then sample the average stressing rate on the 1911 site on the Calaveras fault over 0-10 km depth km depth (the 1984 Morgan Hill mainshock

nucleated at 8 km depth), and find the Calaveras stressing rate at the site of the 1911 shock to be 0.15 ± 0.05 bars/yr, the same value used by Harris and Simpson (1998). The expected delay then comes to 27 ± 9 yr, in agreement with the boundary element calculation. In contrast, Hori and Kaneda (2001) supposed that because of fault creep the stressing rate surrounding the locked 1911 patch could be as high as 1-2 bars/yr, in which case the 1906 stress decrease would have been erased in several years, making the 1911 event more likely.

Given the 15 ± 3 mm/yr Calaveras slip rate, in the absence of the stress changes imparted to the Calaveras by the 1906 shock, the period between 1911 and 1984 nominally accumulated a 1.1 ± 0.2 m slip deficit. A strike-slip $M_w=6.5$ shock has a typical slip of 1.0 m and a rupture area of 29 x 11 km (Wells and Coppersmith, 1994). The 1911 aftershock zone as relocated by Oppenheimer et al. (1990) is about 20 km long, and aftershocks of the 1984 Morgan Hill shock extended for ~ 28 km, with slip occurring over a patchy region of total area 27 x 11 km, in fair agreement with the magnitude estimate provided by our seismic analysis. Thus, a minimum inter-event time of 73 years for the 1911 event is needed to re-accumulate sufficient stress for another $M \sim 6$ shock. If one assumes that the 1911 and 1984 events have typical 30-bar stress drops, then a 4-bar stress drop in 1906 represents about 15% of the total, which would have erased at least 10 yrs of stress accumulation, providing a lower bound on the other estimates we have made. But the 1911 and 1984 shocks could have slipped adjacent or complementary patches of the fault, as occurred during the 1934, 1966, and 2004 Parkfield shocks (Segall and Du, 1993; Murray and Langbein, 2006), in which case the inter-event time for the 1911 event could be much longer than 73 years, and the retardation could similarly be

much longer than 10 years.

Harris and Simpson (1998) invoked rate/state friction of Dieterich (1994) to explain the occurrence of the 1911 earthquake. They posited that if that section of the Calaveras fault would have ruptured in 1908 in the absence of the 1906 earthquake, then the 1906 stress shadow could have delayed the event by only 5 years. This arises because in the theory of rate/state friction, a given stress change has a more modest predicted effect in delaying or advancing the rupture late in an earthquake cycle than if the fault were early in its cycle (Dieterich, 1994). While an intriguing hypothesis, it is essentially untestable.

Dynamic Coulomb stress analysis

While the static Coulomb Failure Function (static-CFF) for numerous earthquakes has been successfully correlated with aftershocks and subsequent mainshocks, Kilb et al. (2002) and Kilb (2003) proposed an alternative parameter to estimate seismic triggering potential, the peak dynamic-CFF change, which is highly sensitive to rupture effects such as directivity. They illustrated this sensitivity by an improved correlation of peak dynamic-CFF with aftershocks for the M=7.3 Landers, CA, earthquake, as compared to static-CFF estimates. In contrast, static-CFF estimates are primarily sensitive to the slip distribution and geometry of the rupture surface.

Here we compare the peak dynamic Coulomb stress changes for the three source models of the 1906 earthquake (Figure 8). Although Thatcher et al (1997) presented a static displacement model, we use it to generate a kinematic rupture model by assuming an epicenter 10 km south of the Golden Gate off Daly City, and a uniform rupture

velocity of 2.7 km/sec. The Coulomb stress changes were computed at 8 km depth in a layered regional model within a 630 km by 260 km area using a fourth-order finite difference method (Olsen, 1994), a friction coefficient of 0.4 and resolved on to vertical faults parallel to the local strike of the Calaveras fault (144°). Reducing the friction to 0.2 has little effect (Figure 9). The Wald et al. and Thatcher et al. source models were implemented using a constant (sub-shear) rupture velocity of 2.7 km/s, as used in the teleseismic modeling of the Wald study. The Song et al. model, on the other hand, used four different rupture velocities along the fault, with a super-shear segment located near the epicenter.

The peak dynamic-CFF distributions shown in Figure 8 for the three source models reveal more strikingly different patterns. Unlike the static-CFF, the peak dynamic-CFF are everywhere positive, and contain significant effects of the rupture propagation, as pointed out by Kilb (2003), with a strong directivity pattern. The most prominent directivity effects occur for the relatively large slip in the Thatcher et al. and Song et al. models toward the north. In contrast, the peak dynamic-CFF values are relatively modest in the epicentral area. The Song et al. model contains smaller peak dynamic-CFF values near the epicenter, to a large extent an effect of the super-shear rupture velocity in this area. At the site of the 1911 earthquake, the peak dynamic-CFF predicted by the Wald et al., Thatcher et al. and Song et al. Models reach ~ 1 bar, 6 bars and 4.5 bars, respectively.

Discussion

Inferences on the 1911 rupture propagation direction

The limited seismic data suggest that the mechanism of the 1911 earthquake may be consistent with right-lateral rupture along the Calaveras fault, similar to the 1984 $M=6.1$ Morgan Hill earthquake. However, the lack of S-waves at teleseismic distances for the Morgan Hill earthquake and the smaller amplitude of its surface waves as recorded at GTT suggest that the 1911 earthquake had a greater magnitude ($6.3 \geq M \geq 6.6$), its direction of rupture propagation was different than the 1984 event, or the data are suspect. Since both GTT and DBN are located along strike to the northwest of the epicenter (Figure 3), unilateral rupture to the southeast in 1984 (Bakun et al., 1984) and toward the northwest in 1911 might explain some of the amplitude differences between seismograms.

Search for historical evidence of 1906 or 1911 Calaveras slip

To learn if the Calaveras fault slipped in response to the 1906 earthquake, we searched for evidence of surface slip or deformation. We searched for astronomic-azimuth measurements that might have been carried out by the Lick Observatory to align its telescope at Mt. Hamilton, which is located 5-10 km north of the 1911 epicenter. We also looked for cultural-offset or geological observations from the contemporary literature, including newspaper accounts of ruptured conduits or offset railways, road or fences, and cadastral surveying measurements for property boundaries. A Southern Pacific railway line crosses the fault obliquely 2.5 km north of Hollister, but no archives of rail repairs from this period exist. The April 20, 1906 edition of the Hollister

newspaper reported that “The big water main on Fifth Street was torn heavily apart, and but for the prompt action of the water company, the town would have been without water.” (The Free Lance, 1906). The Calaveras fault traverses Fifth Street between Powell and West Streets (Rogers and Nason, 1971), but where on Fifth the water main was ruptured was not reported. The water main is likely to have been a buried cast iron pipe, and so fault offset is possible but equivocal. E. C. Templeton reported that at the time of the 1911 shock, “the earthquake cracked the loose gravels at the side of the stream...At one house near here, the most serious damage was the disconnecting of a water pipe at a windmill” on the Coyote Creek 2 km northeast of Edenvale, near the Calaveras fault (Oldenbach, 1911). Although this could be associated with coseismic 1911 slip, it is ambiguous.

Post-1906 creep retardation at Hollister

Unlike the 1911 site, there are surface slip measurements at Hollister ~20 km to the southeast beginning in 1909 (Figure 1b). This reveals a likely 17-year pause in surface creep following the 1906 earthquake, with no change in 1911 (Figure 10). At Hollister a boundary element calculation using the Thatcher et al (1997) model indicates that 0.7 m of left-lateral slip, or a pause in right-lateral creep equivalent to 0.7 m, would have shed the 5 bars of left-lateral stress imposed in 1906 (Figure 7). If the creeping section of the San Andreas fault extending southeast from Hollister slipped postseismically to relieve the 1906-imposed changes, the Calaveras stress drop would reduce to 2.2 bars, and the resulting left-lateral slip needed to relieve the imposed stresses would be 0.5 m (Figure 7). Given the observed 15 ± 3 mm/yr slip rate at Hollister (6.8

mm/yr of which occurs as surface creep) and the 0.5-0.7 m of back slip, a 33-47 yr pause in Hollister creep would be expected, at least twice as long as the observed pause. The 17-year delay at Hollister makes the Hori and Kaneda (2001) explanation for the occurrence of the 1911 earthquake less tenable, because the Hollister creep pause should have also been very short if the stressing rate were in fact as high as 1-2 bars/yr.

Impact of viscoelastic relaxation on Calaveras earthquakes and creep

Viscoelastic relaxation speeds the re-stressing of the Calaveras fault, and thus could contribute to the shortened creep retardation at Hollister, in comparison to purely elastic models. However, viscoelastic recovery does not significantly reload the site of the 1911 earthquake during the 5 years after the 1906 earthquake. Following a 5-bar 1906 stress drop, the stress recovery during the ensuing 5 years at the 1911 epicenter is calculated to be just 0.15 bars using the model of Pollitz et al. (2004) (Figure 11a). In contrast, at the Hollister site viscoelastic rebound is calculated to reach 1.0 bars by 1916, and 2.0 bars by 1926 (Figure 11b). This stress recovery approximately matches well the observed delay in Hollister creep (Figure 10).

The 1911 earthquake could have been triggered by dynamic Coulomb stresses. In support of this contention, we note that the seven aftershocks that occurred between the 1906 mainshock and the 1911 Calaveras earthquake all struck where the dynamic Coulomb stress exceeded 3 bars (Figure 12). Nevertheless, this test is less stringent than for the static stress change since most of the peak dynamic stress changes are only positive. In addition, aftershocks were not recorded, or did not occur, in many of the regions with the highest peak dynamic stress changes, and so there is no correlation

between aftershock frequency or magnitude with peak dynamic Coulomb stress (Figure 12). The absence of a correlation may be the product of the impoverished aftershock catalog. Finally, the time delay in dynamic triggering is not readily explained, although a rate/state friction explanation has been proposed by Parsons (2005).

Conclusions

First motion, body wave and teleseismic surface wave analysis for the first time permits a focal mechanism analysis of the 1911 Calaveras earthquake. We find that it was most likely a $M \sim 6.5$ right-lateral event on the Calaveras fault. Our mechanism, location, and magnitude are consistent with assumptions made by Oppenheimer et al. (1990), Harris and Simpson (1998), and Bakun (1999), but inconsistent with Jaumé and Sykes (1996), who suggested that it was a reverse mechanism located east of the Calaveras fault, and likely inconsistent with Hori and Kaneda (2001), who proposed a fault stressing rate that is too high to explain the Hollister creep pause. The mechanism and location of the 1911 shock means that it struck on a fault in the stress shadow of the 1906 earthquake, and thus cannot be easily reconciled with the static Coulomb stress hypothesis.

The 1911 earthquake occurred only about a quarter-way through an expected retardation of about 25 yr caused by the 1906 earthquake, and viscoelastic re-stressing would have only shortened this by a small amount. Thus, the best explanation for the occurrence of the 1911 shock is that it was instead promoted by the peak dynamic Coulomb stress imparted by the 1906 earthquake.

We also find that creep retardation did occur at Hollister, just 20 km to the

southeast on the Calaveras fault, which also lies in the stress shadow of the 1906 earthquake. The creep retardation of 17 years can be well explained by the coseismic stress drop, postseismic San Andreas creep, and viscoelastic recovery. Thus the creep retardation provides evidence in support of the static Coulomb hypothesis. Hollister has peak dynamic-CFF of 2 bars for the Wald et al. 1906 model, 10 bars for Thatcher et al., and 8 bars for Song et al., and thus if creep were also driven by dynamic stresses, the creep should have accelerated rather than paused.

Acknowledgments. We would like to thank Elliot Grunewald, Lee Rosenberg, Willie Lee and John Ebel for their assistance in locating seismograms and other historical information. We would also like to thank seismograph station managers around the world who maintain and helped us recover the 1911 and 1984 seismograms.

References

- Baker, M.R., and D.I. Doser (1988). Joint inversion of regional and teleseismic earthquakes waveforms, *J. Geophys. Res.* 93, 2037-2045.
- Bakun, W.H., (1999). Seismic activity of the San Francisco Bay region, *Bull. Seismol. Soc. Amer.* 89, 764-784.
- Bakun, W.H., M.M Clark, R.S. Cockerham, W.L. Ellsworth, A.G. Lindh, W.H. Prescott, A.F. Shakal, and P. Spudich (1984). The 1984 Morgan Hill, California, earthquake, *Science*, 225, 228-291.
- Dieterich, J., A constitutive law for rate of earthquake production and its application to earthquake clustering, *J. Geophys. Res.*, 99, 2601-2618, 1994.
- Doser, D.I., and S.R. VanDusen (1996). Source processes of large ($M \geq 6.5$) earthquakes of the southeastern Caribbean (1926-1960), *Pure Appl. Geophys.* 146, 43-66.
- Ellsworth, W.L. (1990). Earthquake history, 1769-1989, *The San Andreas Fault System, California*, R.E. Wallace (Editor), Chap. 6, U.S. Geol. Surv. Profess. Pap. 151, 153-

188.

- Felzer, K.R. and E.E. Brodsky (2005). Testing the stress shadow hypothesis, *J. Geophys. Res.* 110, doi:10.1029/2004JB003277.
- Gutenberg, B., and C.F. Richter (1985). *Seismicity of the Earth and Associated Phenomena*, 2nd ed., Princeton University Press, Princeton, New Jersey, 310 pp.
- Harris, R.A., and R.W. Simpson (1998). Suppression of large earthquakes by stress shadows: A comparison of Coulomb and rate-and-state failure, *J. Geophys. Res.* 103, 24,439-24,451.
- Hori, T., and Y. Kaneda (2001). A simple explanation for the occurrence of the 1911 Morgan Hill earthquake in the stress shadow of the 1906 San Francisco earthquake, *Geophys. Res. Lett.* 28, doi:10.1029/2000GL012727.
- Jaumé, S.C., and L. R. Sykes (1996). Evolution of moderate seismicity in the San Francisco Bay region, 1950 to 1993: Seismicity changes related to the occurrence of large and great earthquakes, *J. Geophys. Res.* 101, 765-789.
- Kilb, D., J. Gomberg, and P. Bodin (2002). Aftershock triggering by complete Coulomb stress changes, *J. Geophys. Res.*, 107, doi:10.1029/2001JB000202.
- Kilb, D. (2003). A strong correlation between induced peak dynamic Coulomb stress change from the 1992 *M*7.3 Landers, California, earthquake and the hypocenter of the 1999 *M*7.1 Hector Mine, California, earthquake, *J. Geophys. Res.* 108, doi:10.1029/2001JB000678.
- Manaker, D.M., A.J. Michael and R. Burgmann (2005). Subsurface structure and kinematics of the Calaveras-Hayward fault stepover from three-dimensional V_p and seismicity, San Francisco Bay region, California, *Bull. Seismol. Soc. Amer.* 95, 446-470.
- Meltzner, A.J., and D.J. Wald, (2003). Aftershocks and Triggered Events of the Great 1906 California Earthquake, *Bull. Seismol. Soc. Amer.* 93, 2160–2186., 2003.
- Murray, J., and J. Langbein (2006). Slip on the San Andreas Fault at Parkfield, California, over Two Earthquake Cycles, and the Implications for Seismic Hazard, *Bull. Seismol. Soc. Amer.* 96, S283–S303.
- Oldenbach, F.L. (1911). Notes on the California earthquake of July 1, 1911, *Bull. Seismol. Soc. Am.* 1, 110-121.

- Oppenheimer, D.H., W.H. Bakun, and A.G. Lindh (1990). Slip partitioning of the Calaveras fault, California, and prospects for future earthquakes, *J. Geophys. Res.* 95, 8483-8498.
- Olsen, K.B. (1994). Simulation of three-dimensional wave propagation in the Salt Lake Basin, University of Utah (PhD thesis).
- Parsons, T., A hypothesis for delayed dynamic earthquake triggering, *Geophys. Res. Lett.*, 32, L04302, doi:10.1029/2004GL021811, 2005.
- Parsons, T., Tectonic stressing in California modeled from GPS observations, *J. Geophys. Res.*, 111, B03407, doi:10.1029/2005JB003946, 2006.
- Pollitz, F., W.H. Bakun and M. Nyst (2004). A physical model for strain accumulation in the San Francisco Bay region; stress evolution since 1838, *J. Geophys. Res.* 109, doi:10.1029/2004JB003003.
- Rogers, T.H., and R.D. Nason (1971). Active displacement on the Calaveras fault zone at Hollister, California, *Bull. Seismol. Soc. Am.* 61, 399-416.
- Segall, P., and Y. Du (1993). How similar were the 1934 and 1966 Parkfield earthquakes?, *J. Geophys. Res.*, 98, 4527-4538.
- Simpson, R. W. and P. A. Reasenberg, Earthquake-induced static-stress changes on central California faults, *U.S. Geol. Surv. Prof. Pap.* 1550-F, 55-89, 1994.
- Song, S.-G., Gregory C. Beroza, G.C., and P. Segall (2007). A unified source model for the 1906 San Francisco earthquake, *Bull. Seismol. Soc. Amer.*, in press.
- Stein, R.S., (1999). The role of stress transfer in earthquake occurrence, *Nature* 402, 605-609.
- Templeton, E.C. (1911). The central California earthquake of July 1, 1911, *Bull. Seismol. Soc. Am.* 1, 167-169.
- Thatcher, W., Marshall, G., and M. Lisowski (1997). Resolution of fault slip along the 470-km-long rupture of the great 1906 San Francisco earthquake and its implications, *J. Geophys. Res.* 102, 5,353-5,367.
- The Free Lance (1906). Earthquake! Havoc and destruction wrought in a few seconds; Hollister's loss is \$250,000, Hollister, Calif. newspaper, vol. XXIII, No. 16, 20 April 1906.
- Toda, S., and R. S. Stein (2002). Response of the San Andreas Fault to the 1983

- Coalinga-Nuñez Earthquakes: An Application of Interaction-based Probabilities for Parkfield, *J. Geophys. Res.* 107, 10.1029/2001JB000172.
- Topozada, T.R. (1984). History of earthquake damage in Santa Clara County and comparison of 1911 and 1984 earthquakes, in *The 1984 Morgan Hill, California Earthquake*, J.H. Bennett and R.W. Sherburne (Editors), Calif. Div. Mines Geol. Spec. Publ. 68, 237-248.
- Wald, D.J., H. Kanamori, D.V. Helmberger, and T.H. Heaton (1993). Source study of the 1906 San Francisco earthquake, *Bull. Seismol. Soc. Am.* 83, 981-1019.
- Wells, D.L., and K.J. Coppersmith (1994). New empirical relationships among magnitude, rupture length, rupture width, rupture area, and surface displacement, *Bull. Seismol. Soc. Am.* 84, 974-1002.
- Wood, H.O (1912a). On the region of origin of the central Californian earthquakes of July, August and September, 1911, *Bull. Seismol. Soc. Am.* 2, 31-39.
- Wood, H.O. (1912b). The registration of earthquakes at the Berkeley station from April 1 to September 30, 1911 and at the Lick Observatory station from May 23 to September 30, 1911, *Bull. Of the Seismographic Stations No. 2*, Univ. of Calif. Publications, 11-48.
- U.S. Geological Survey (2007). California Reference Geologic Fault Parameter Database, compiled by the USGS, CGS, SCEC Working Group for California Earthquake Probabilities, (<http://gravity.usc.edu/WGCEP/resources/data/refFaultParams/index.html>), U.S. Geol. Surv. Open-File Rep., submitted.
- Wald, D.J., Kanamori, H., Helmberger, D.V., and T.H. Heaton (1993), Source Study of the 1906 San Francisco Earthquake, *Bull. Seism. Soc. Am.* 83, 981-1019.

Department of Geological Sciences
University of Texas at El Paso
El Paso, TX 79968
(D.I.D.)

U.S. Geological Survey, MS 977
345 Middlefield Road
Menlo Park, CA 94025
(R.S.S.; F.P.)

Active Fault Research Center
Advanced Institute of Science and Technology
Higashi 1-1
Tsukuba 305-8567, Japan
(S.T.)

Department of Geological Sciences
San Diego State University, MC1020
San Diego, CA 92182-1020
(K.B.O.)

Table 1 – Instrument Response Information

Instrument	Seismometer period (sec)	Damping	Magnification
GTT NS (1911) astatic pendulum	12.2	4	160
GTT EW (1911) astatic pendulum	12.2	3.5	159
GTT NS (1984) astatic pendulum	9.4	2.8	153
GTT EW (1984)	10.3	3.5	157
DBN EW (1911) Wiechert	5	4	170
DBN NS (1911) Wiechert	5	4	170
DBN EW (1984) Galitzin	25	---	310
DBN NS (1984) Galitzin	25	---	310
SLM NS (1911) Wiechert	8	5	200
SLM EW (1911) Wiechert	8	5	200

Abbreviations: GTT= Göttingen, DBN=Debilt, SLM=St. Louis, Missouri

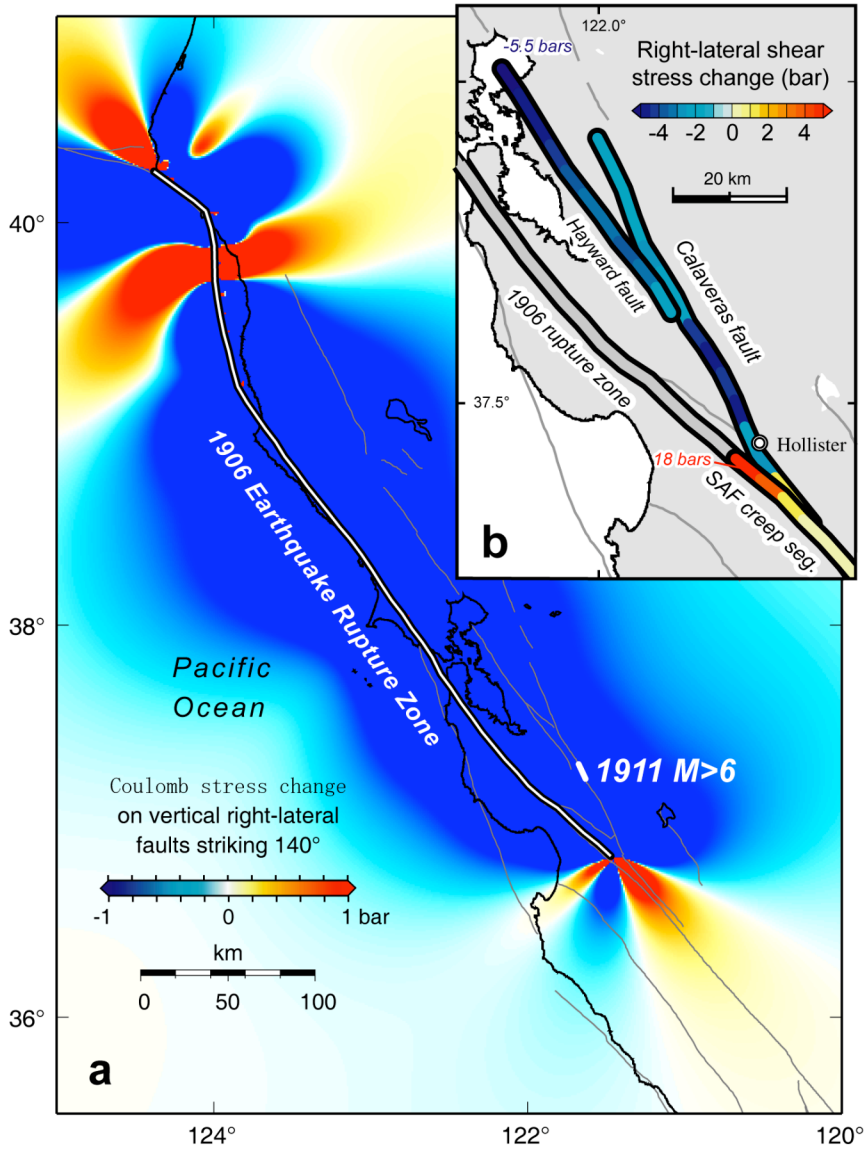


Figure 1 – (a) Map showing static Coulomb stress change imparted by the 1906 earthquake (using the model of Thatcher et al, 1997) on vertical right-lateral strike slip faults striking 140°. (b) Right-lateral shear stress change resolved on the Hayward, Calaveras faults, and creeping segment of the San Andreas fault (SAF). In this calculation, the local strike of the receiver fault is used, rather than a common strike.

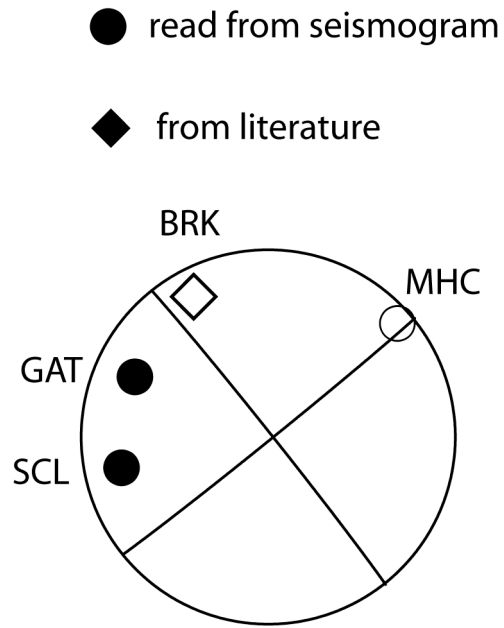


Figure 2 – First motions observed for the 1911 Calaveras earthquake. Open symbols are dilatations, solid symbols are compressions.

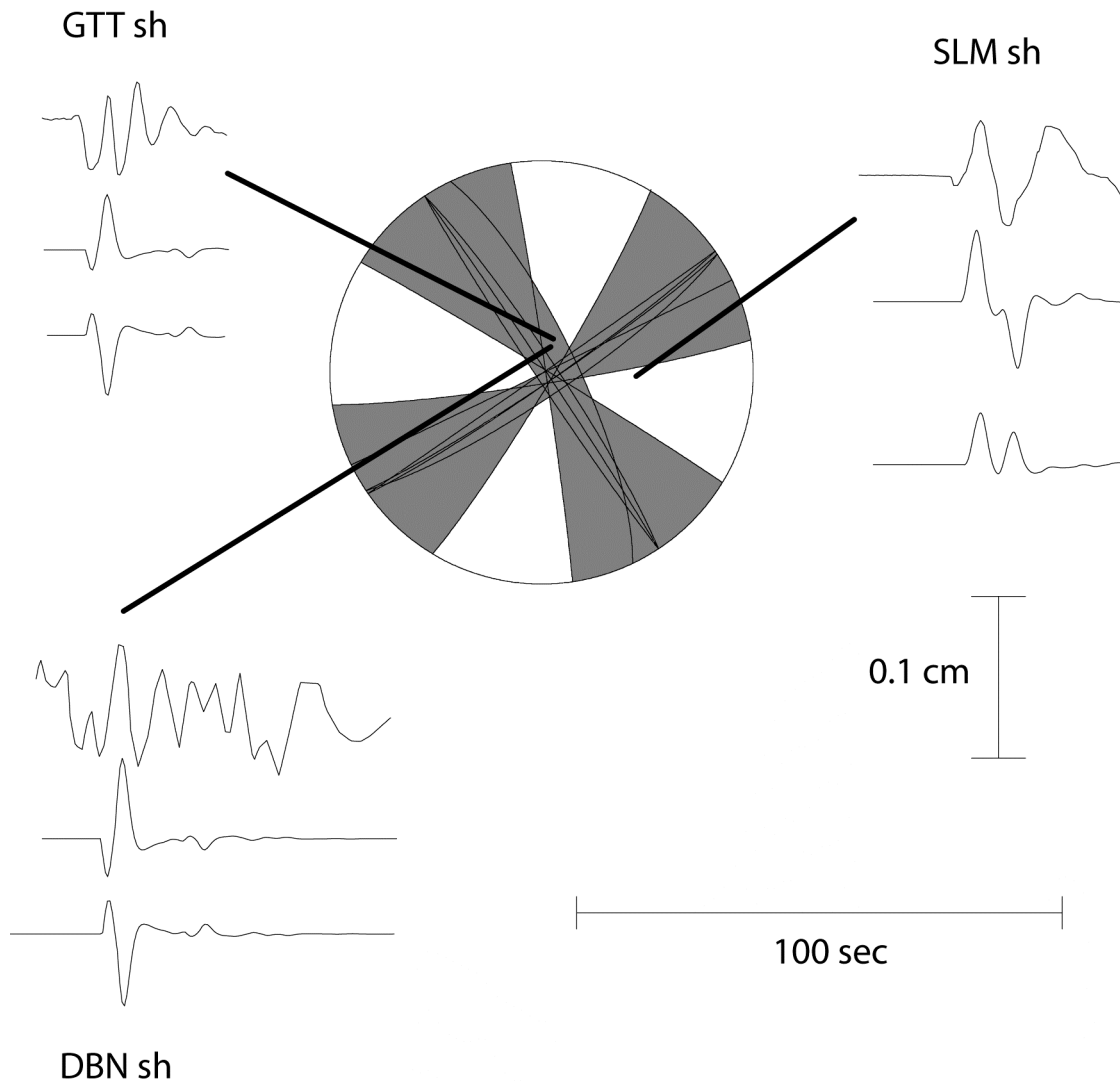


Figure 3 - Results of waveform modeling. Top seismogram of each group is observed, middle seismogram is synthetic for right-lateral strike-slip mechanism similar to 1984 Morgan Hill earthquake, bottom seismogram is synthetic for reverse mechanism (see text for details). Grey areas reflect the range of focal mechanisms that can fit the observed waveforms assuming a strike-slip mechanism.

a)

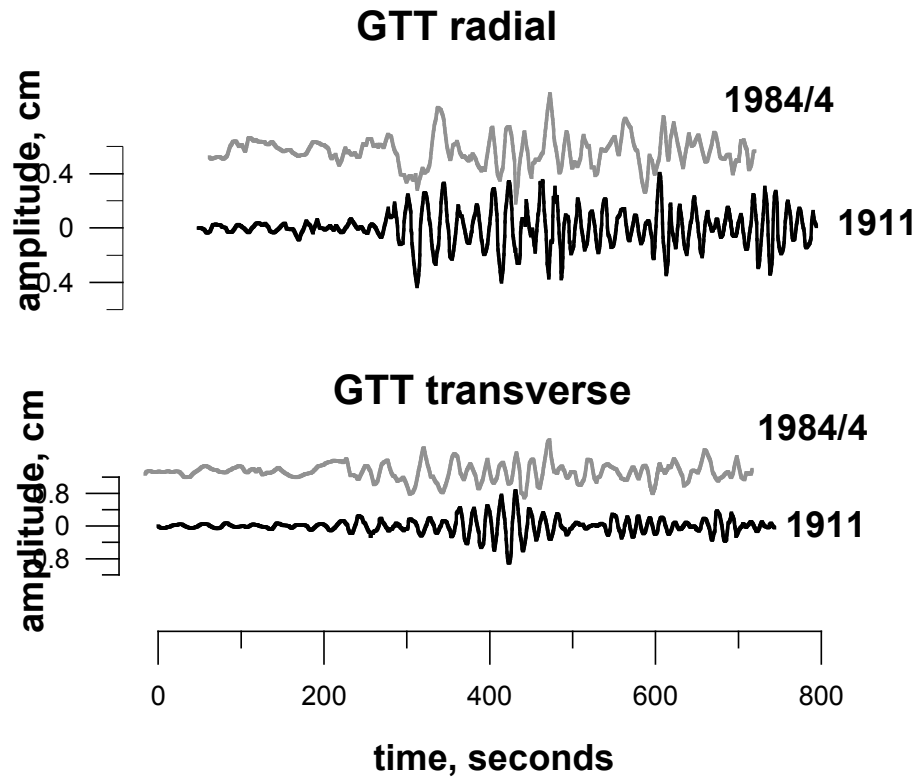


Figure 4 (see b).

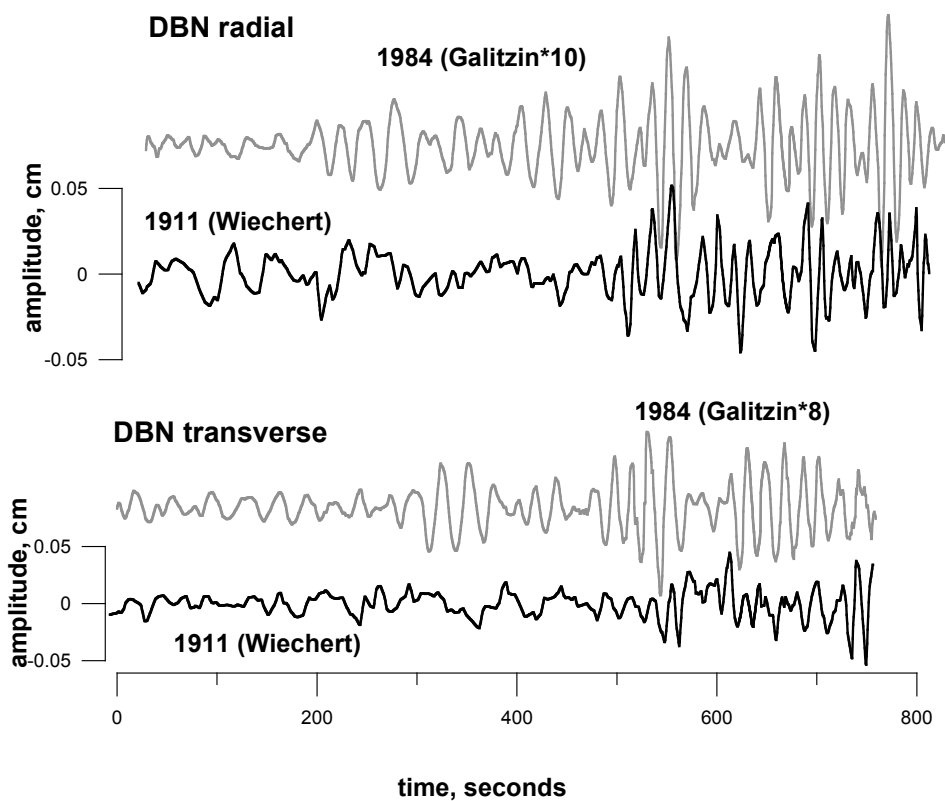
b)

Figure 4- Comparison of surface waves recorded at GTT (a) and DBN (b) for the 1911 (black lines) and 1984 (gray lines) earthquakes. For GTT the 1984 seismograms are a factor of 4 smaller than the amplitude scales indicated. For DBN the 1984 seismograms are a factor of 8 to 10 larger than the amplitude scales indicated. Note that there are differences in instrumentation between 1911 and 1984 at DBN (see Table 1).

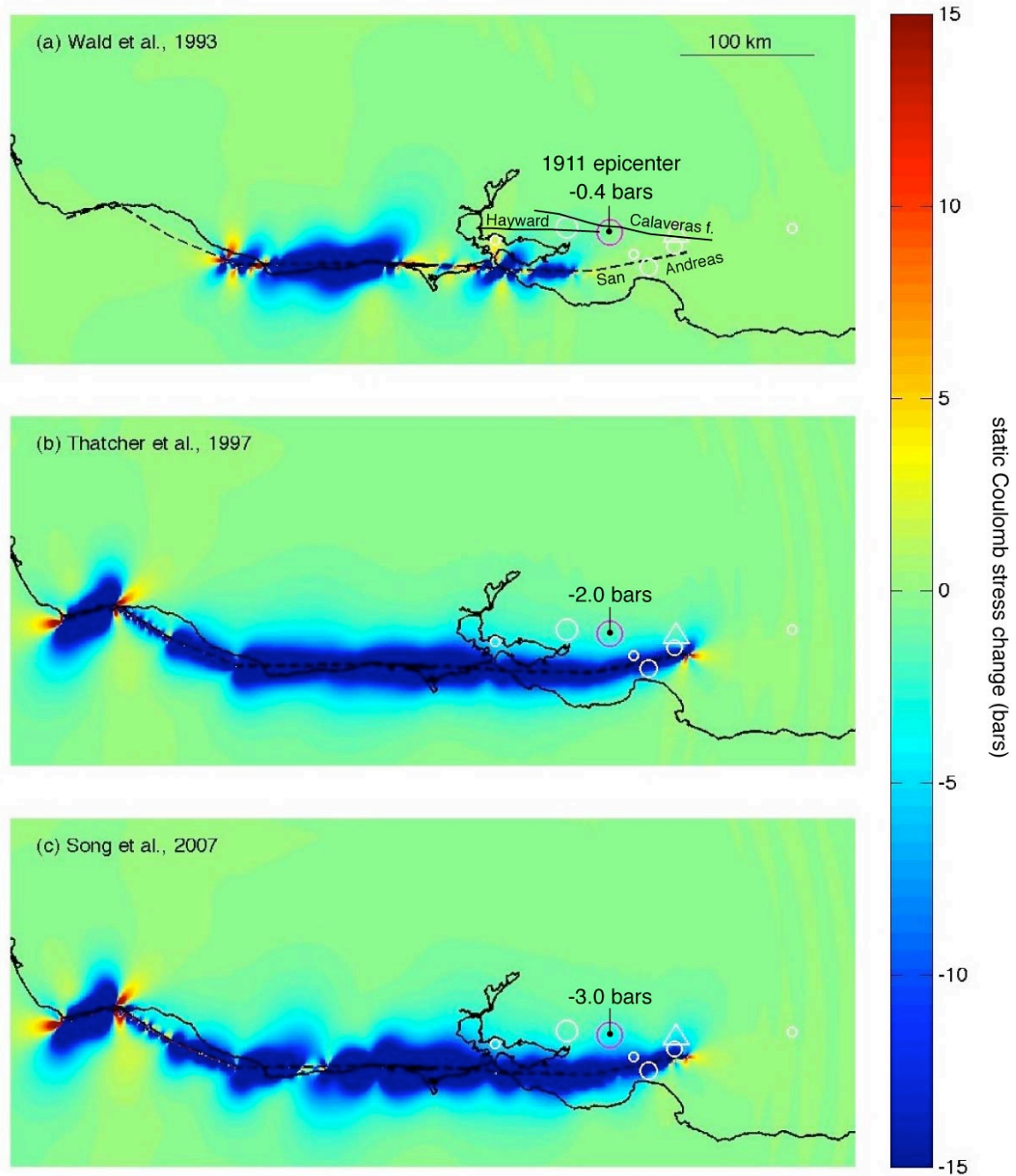


Figure 5 – The static Coulomb stress at 8 km depth imparted by the 1906 quake using slip models by (a) Wald et al. (1993), (b) Thatcher et al. (1997), and (c) Song et al. (2006), assuming a 0.4 friction coefficient on vertical receiver faults striking 144° . The triangle depicts the location of Hollister, the magenta circle marks the 1911 epicenter, and other 1906-1911 aftershocks from Meltzner and Wald (2003) are white, with circle size proportional to magnitude.

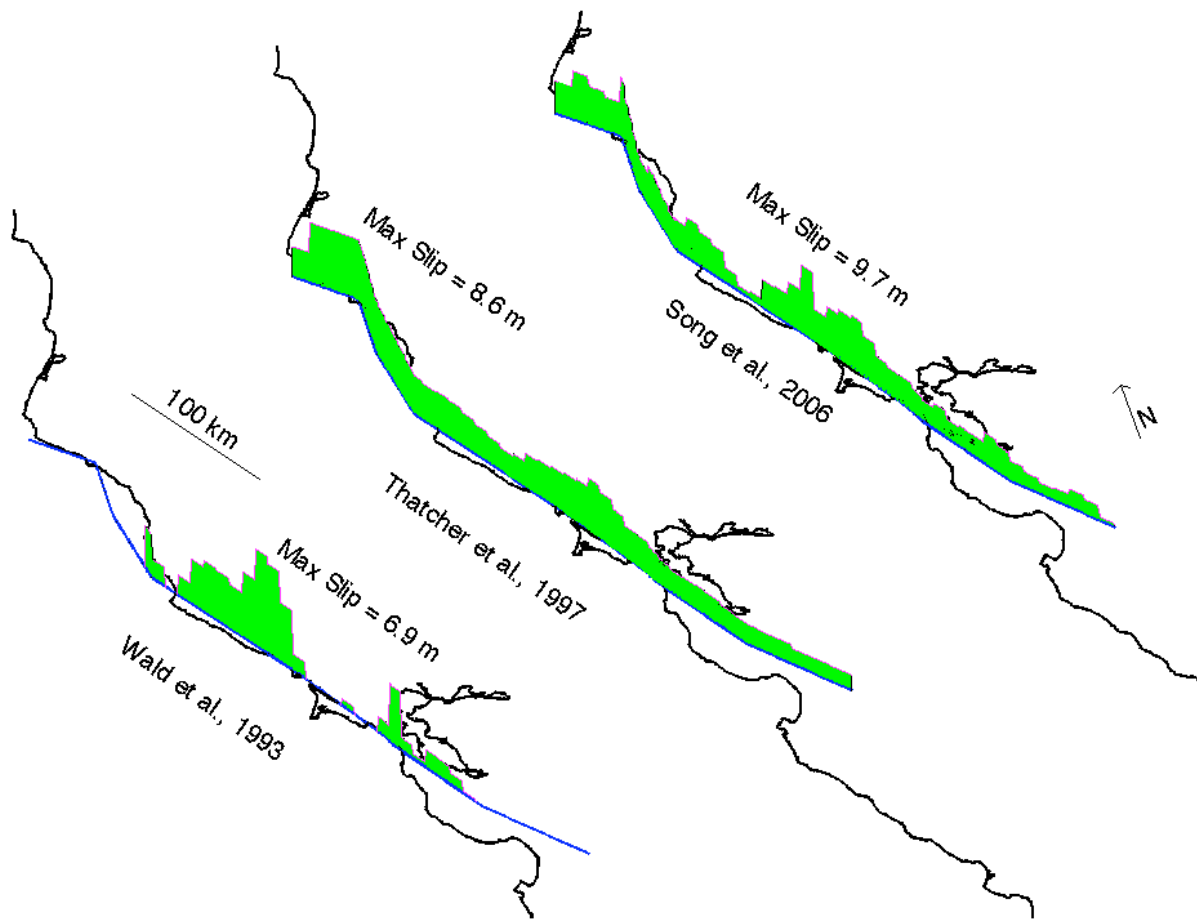


Figure 6 – Comparison between the slip models for the 1906 event by Wald et al. (1993), Thatcher et al. (1997) and Song et al. (2006).

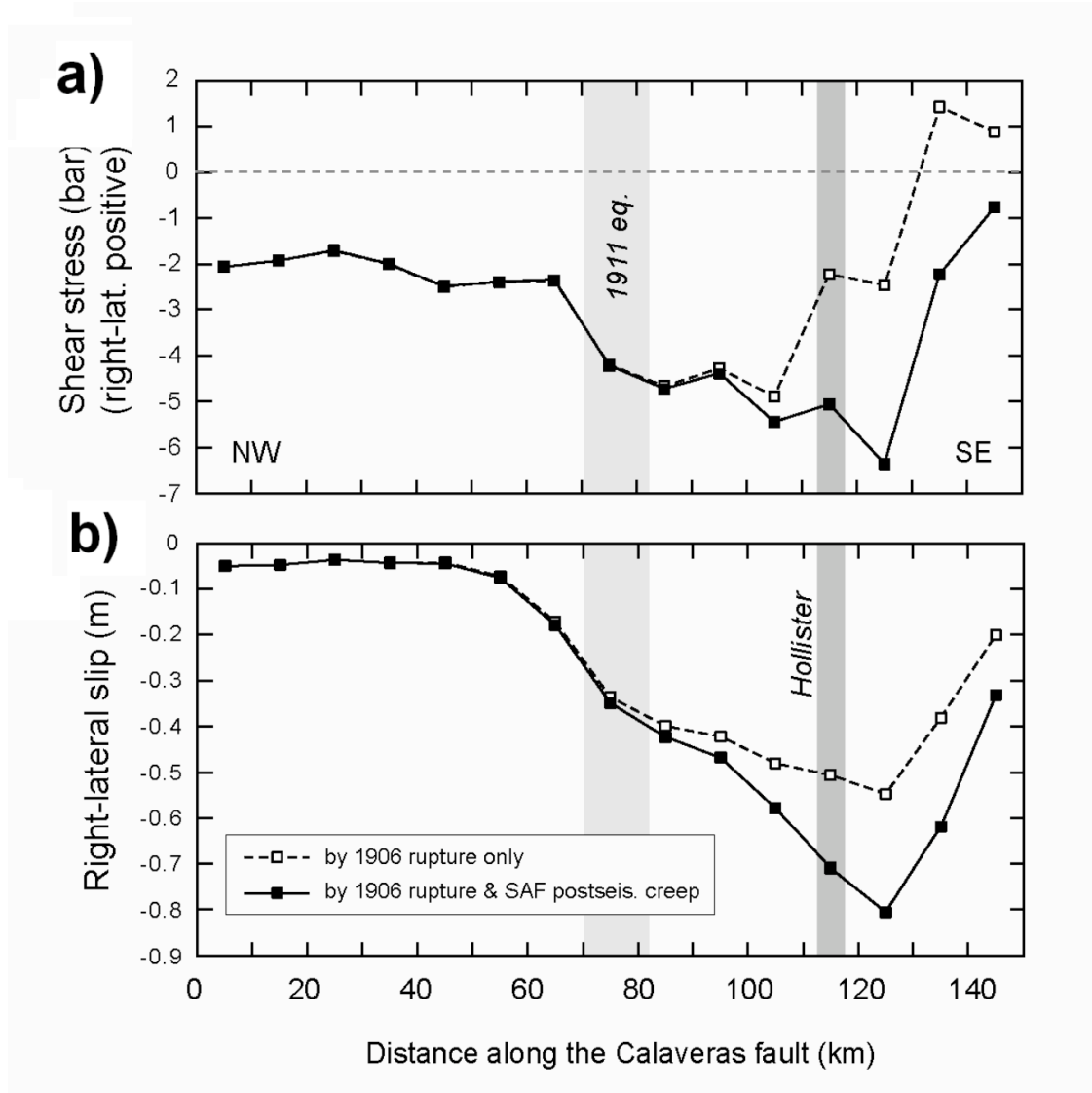


Figure 7 – (a) Shear stress in bars imposed by 1906 earthquake on the Calaveras fault, using the Thatcher et al (1997) model. This is shown graphically in Figure 1b. (b) Right-lateral slip required to shed stress imposed by 1906 earthquake (bottom). Shaded gray areas indicate locations of the 1911 earthquake and Hollister.

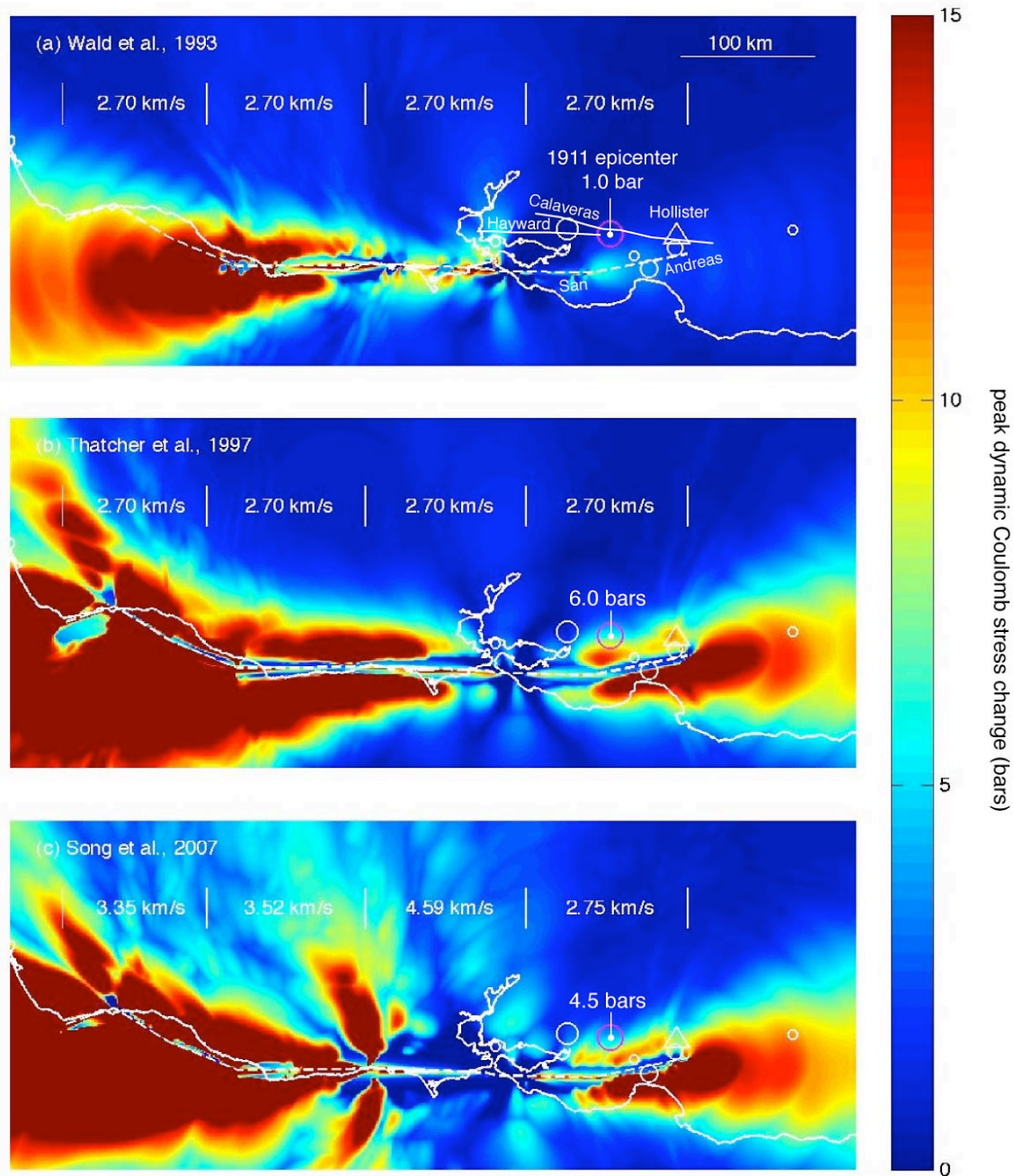


Figure 8 – Peak dynamic Coulomb stress distributions generated by the (a) Wald et al. (1993), (b) Thatcher et al. (1997), and (c) Song et al. (2006) source models. The spatially-variable rupture speed is shown for each model. Receiver fault friction is assumed to be 0.4, and symbols are as in Figure 5. Note that the stress scale ranges over 0-15 bars; blue does not represent a stress decrease as it does in Figure 6.

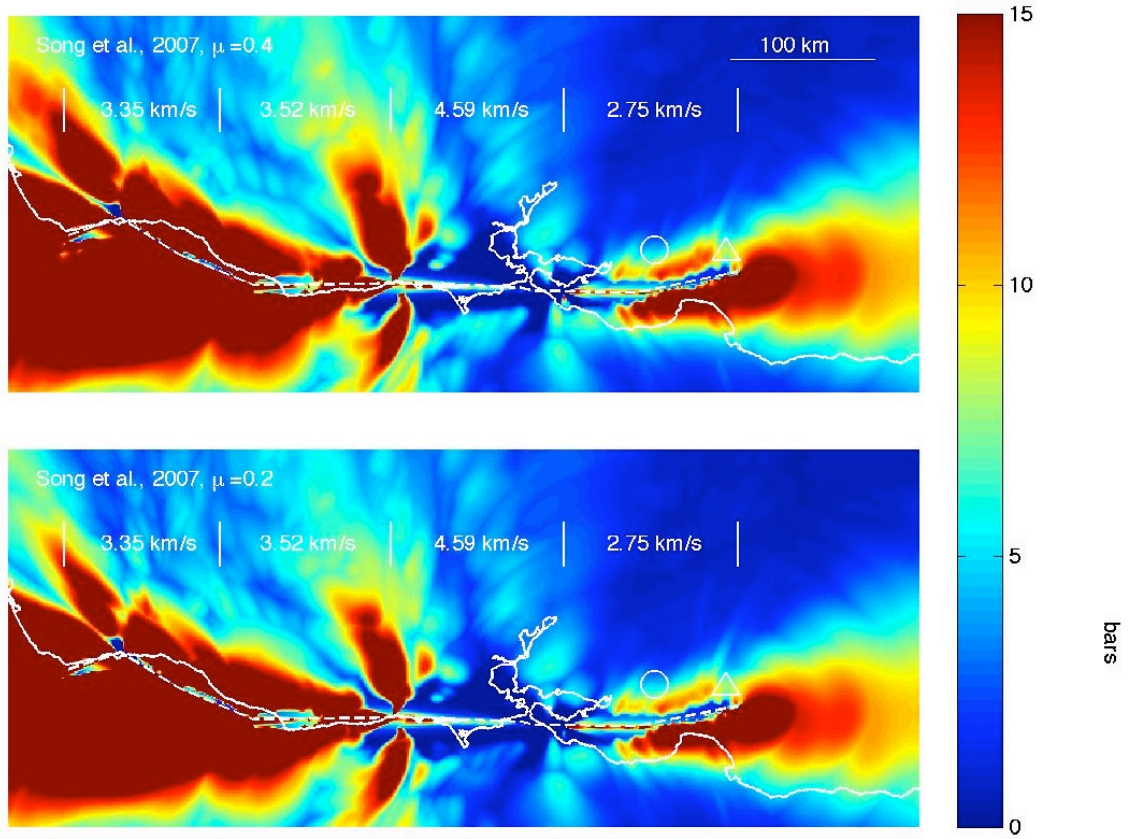


Figure 9. The effect on the peak dynamic Coulomb stress of lowering the assumed friction coefficient on receiver faults from 0.6 (Figure 8) to 0.4 to 0.2 here is modest.

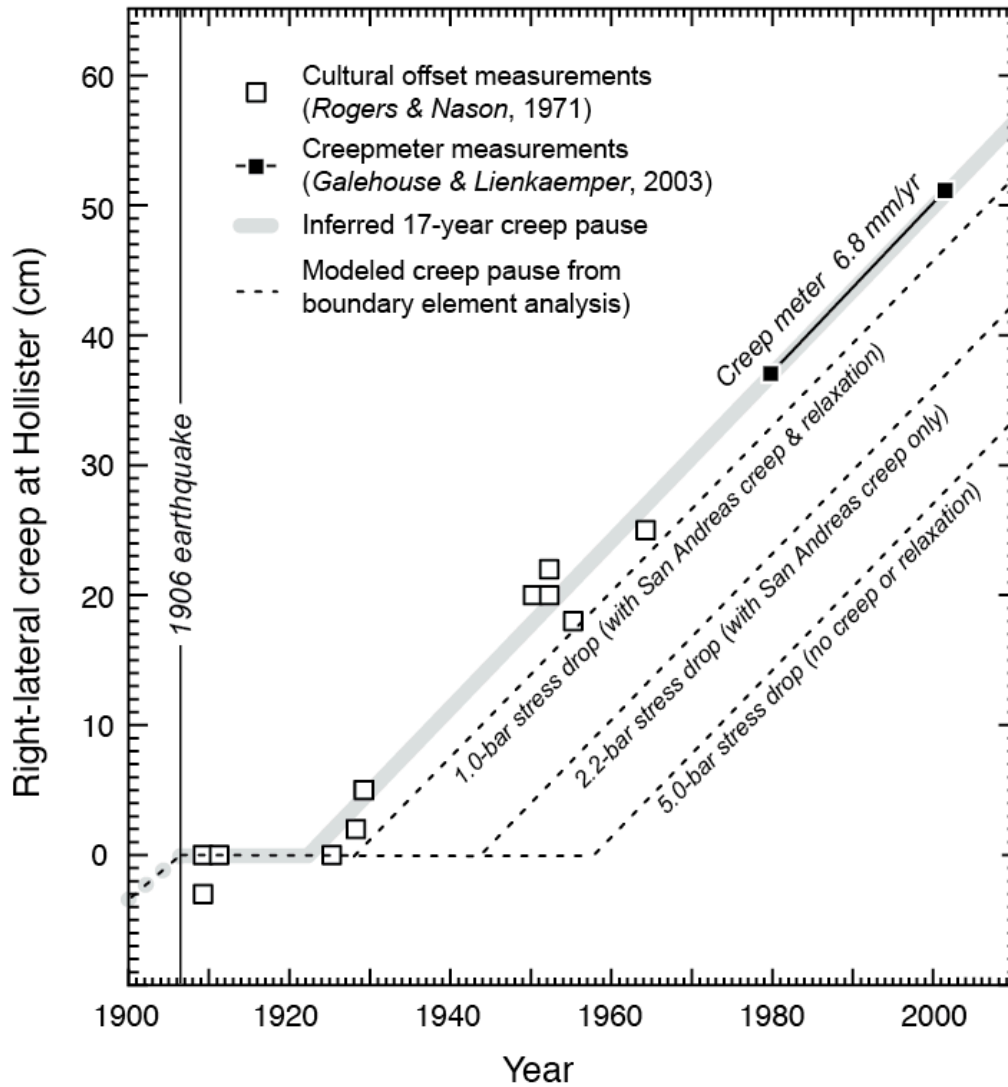


Figure 10 – Creep models compared to creep data (boxes and solid line) observed at Hollister since 1910. Gray line indicates inferred 17-year creep pause and dashed lines indicate creep retardation models for 2-5 stress drop in 1906.

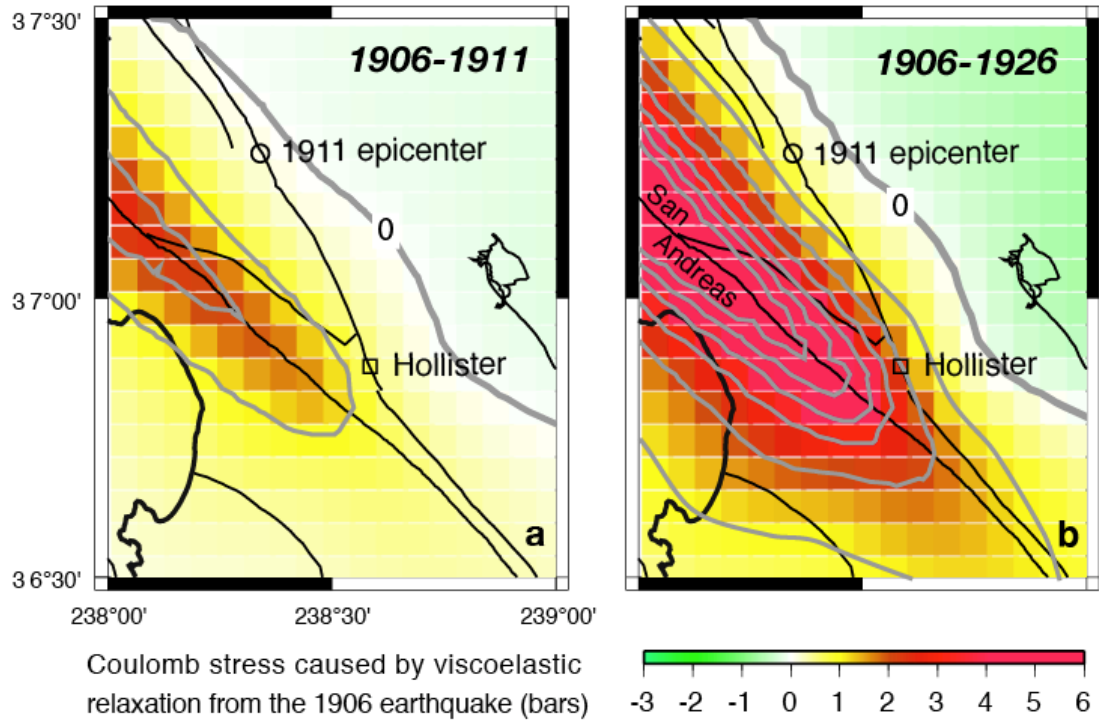


Figure 11. Fault re-stressing associated with relaxation caused by the 1906 earthquake for two time periods, (a) at the time of the 1911 Calaveras earthquake (+0.2 bars); and (b) within several years of the end of the creep pause at Hollister (+2.0 bars).

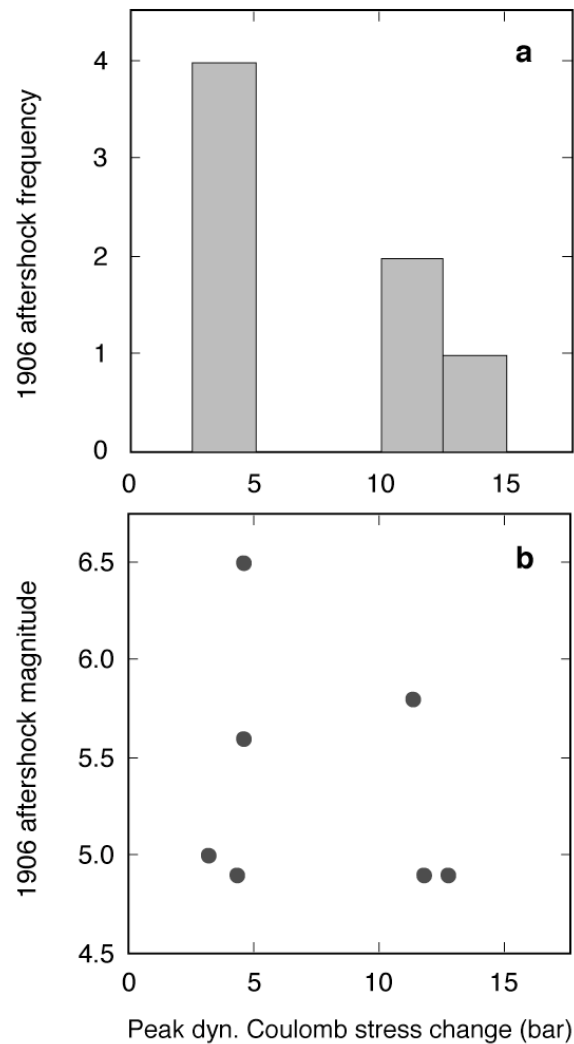


Figure 12. 1906 aftershock frequency (a) and magnitude (b) as a function of calculated peak dynamic Coulomb stress change. Aftershocks from Meltzner and Wald (2003) during the first five years after 1906 are included, their fault planes are assumed to be parallel to the San Andreas fault, the Song et al (2007) source model for the 1906 earthquake is used, and a friction coefficient of 0.6 is assumed. Although no positive correlation is observed in either case, all shocks occurred where the peak dynamic Coulomb stress exceeded 3 bars.